ORIGINAL RESEARCH

Effect of starch-based flame retardant on the thermal degradation and combustion properties of reconstituted tobacco sheet

Ning Shao · Yaqing Qu · Li Hou · Yonghua Hu · Zhengfeng Tian · Yun Gao · Xiaolan Zhu

Abstract In this paper, starch, distarch phosphate (DSP) and hydroxypropyl distarch phosphate (HPDSP) were used as "green" carbon sources with ammonium polyphosphate (APP) to prepare flame retardant reconstituted tobacco sheet (RTS) by paper-making process and the effect of these starch-based flame retardants on their thermal degradation and combustion properties was preliminarily investigated. Micro-scale combustion calorimetry results showed the value of the heat release of modified RTS was lower than that of pure RTS, demonstrating the restrained combustion behavior of modified RTS. TG-FTIR and TG-MS analysis indicated that the starch-based flame retardant coating promoted the char formation, inhibited char combustion and release of gaseous products except for NH_3, with the relative best comprehensive performance of APP-DSP. Cigarette burning cone analysis also confirmed that the modified RTS had lower temperature and smaller burning cone volume than that of pure RTS, especially APP-HPDSP-RTS. This work could highly expand the application of starch and its derivatives in flame retardant and tobacco industry.

N. Shao · Y. Qu · L. Hou · Y. Gao · X. Zhu (✉)
The USTC-Anhui Tobacco Joint Laboratory of Tobacco Chemistry, Research Center of Tobacco and Health, University of Science and Technology of China, Hefei 230052, China
e-mail: zxl8906@ustc.edu.cn

Y. Hu (✉) · Z. Tian
The USTC-Anhui Tobacco Joint Laboratory of Tobacco Chemistry, Center of Technology, China Tobacco Anhui Industrial Corporation, Hefei 230088, China
e-mail: hchem600@sina.com
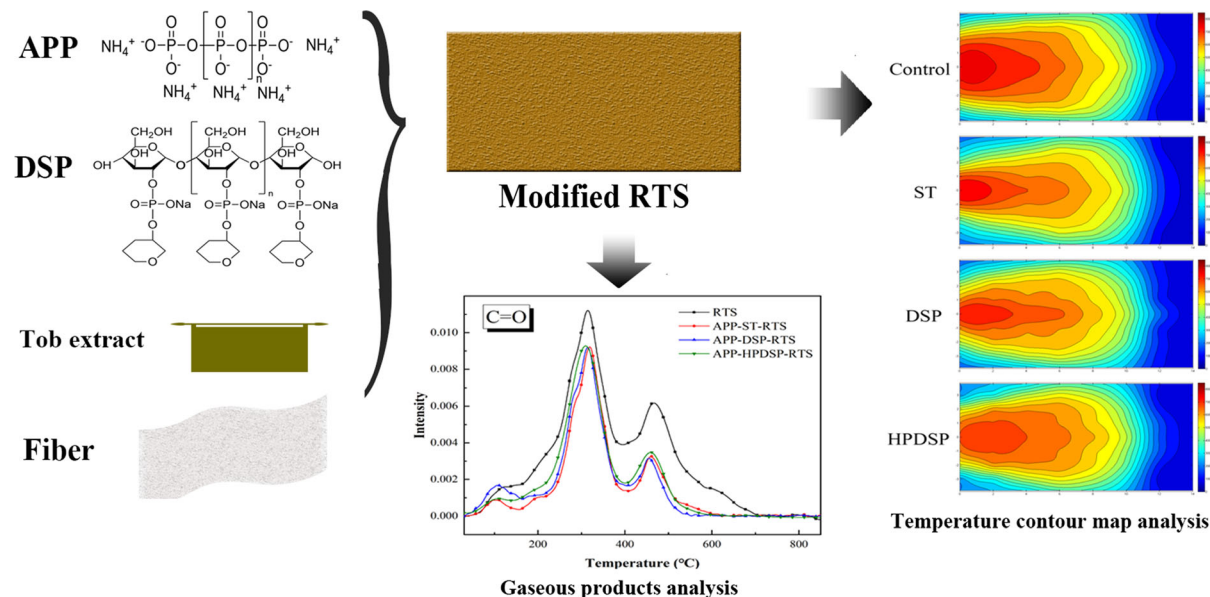
Graphic abstract

Introduction

Intumescent flame retardant (IFR) coating technology had been widely used in material field for offering an efficient flame retardancy to matrix including steel, woods and polymers in the past 30 years (Shi and Wang 2016; Zhao et al. 2020). Many various IFRs have been applied to modify the combustion characteristics of cotton-based fabrics (Chen et al. 2015b; Yan et al. 2018; Wang et al. 2019). Typically, IFR has three active ingredients, including carbon, acid and gas sources. Carbonization agent is the basis component of IFR, taking a vital effect on the formation of char that can be used as an obstacle to hinder the combustion of materials (Liu et al. 2018). A great deal of research has emerged in recent years about different carbonization agents, such as polyamide (Li et al. 2017) and pentaerythritol (Wang et al. 2017; Liu et al. 2020). However, these carbonization agents root in petroleum that is a limited resource, and the processing procedure is harmful to environment. With the increasing concern on environment and resource

around the world, biodegradable alternatives originated from renewable sources have gained increasing popularity since they can make us free from our dependence on petroleum-based products (Wang et al. 2020; Liu et al. 2020).

Starch (ST) is one of the most popular renewable and biodegradable polymers due to its versatility, abundance and biodegradability (Chen et al. 2020). Much attention has been paid to its modification on biomedical and ecological application in the past decades. Generally, native starch can be converted into thermoplastic starch in the presence of plasticizer (such as water). This unique property makes it a potential alternative in the field of food, textile, paper making and other industries (Shen et al. 2014; Wang et al. 2015; Oltramari et al. 2017). Besides, ST can be cross-linked with phosphate to form chemical modified ST, such as distarch phosphate (DSP), hydroxypropyl distarch phosphate (HPDSP) to improve its solubility, swelling capacity (Passauer et al. 2009). Moreover, starch and its derivatives (such as DSP, HPDSP) have the potential to be used as carbonization agent due to their structure of multi-hydroxyl group (Hamadache et al. 2019). On the other hand, ammonium polyphosphate (APP) has been widely used as acid source to yield polyphosphoric acid on heating and cooperate with carbon source to form an intumescent flame retardant system promoting char

formation (Lin et al. 2018; Schirp and Hellmann 2019; Zeng et al. 2020; Zhang et al. 2020). Therefore, APP, ST and its derivatives have the potential to work as IFR synergistically in application.

Tobacco smoke is widely acknowledged as a leading cause of illness and death and it has been an important and long-term task for tobacco scientists and technicians to reduce its harm to human health. The pyrolysis and combustion of tobacco release thousands of harmful substances, including tobacco-specific nitrosamines (TSNAs), carbon monoxide, polycyclic aromatic hydrocarbons (PAHs), carbonyl compounds, and phenols. (Talhout et al. 2011). Moreover, burning temperature of cigarette has a significant impact on toxicity of smoke. More and more research has shown that there is a highly close association of yields of harmful substances in smoke with thermal degradation and burning characteristics of tobacco (Takahashi et al. 2018; Safdari et al. 2019). Therefore, modifying tobacco combustion and pyrolysis and lowering burning temperature of cigarette are very important to reduce the hazard of tobacco products. Reconstituted tobacco sheet (RTS) was produced usually by tobacco dust, stem, leaf, scraps and so on, which cannot be incorporated directly in cigarettes. The addition of RTS to cut tobacco not only brings out its apparent economic benefits on the manufacturing of cigarettes but also reduces the health risks of smoking (Zhou et al. 2017). Generally, the water soluble and insoluble fractions of tobacco wastes are separated through extraction. The soluble extracts are concentrated to paste, while insoluble residues are made into paper by papermaking or other methods. Finally, the tobacco based paper is immersed with the condensed tobacco extract to get RTS (Wang et al. 2014). The incorporation of natural fiber like softwood pulp makes RTS becomes a "special textile" (Chen et al. 2014b). Due to the advantage of low cost, RTS has been widely used as filler in cigarette products to regulate the combustion behavior. Furthermore, unlike its origin-tobacco, it is quite easy to control the processing technology of RTS based on mechanical strength and composition requirements.

Additives modifying RTS during process have become a research direction in cigarette industry. These additives can change the thermal degradation and combustion behavior of RTS, further influence the formation of gaseous products and therefore regulate contents of harmful products. In fact, salt and catalyst are common additives for RTS. For example, Gao et al. studied the effects of sodium and potassium citrate on the properties of RTS, such as major chemical composition, surface microstructure, release of tar and carbon monoxide (CO). It concluded that potassium citrate can accelerate thermal degradation in 200–400 °C and decrease the amount of tar and CO significantly (Gao et al. 2015). Chen et al. (2014a) found that the carbonyl compounds were originated from the decomposition of saccharides during RTS combustion, while CO mainly came from the incomplete combustion of carbonized char. Calabuig et al. (2019) reported the addition of catalyst SBA-15 could cut down the release of CO at high temperature. Deng et al. (2016) fabricated an eco-friendly layer-by-layer (LbL) assemblies of chitosan/APP nanocoatings on polysiloxane foam successfully and exhibited the effect on flame retardancy and smoke suppression of the coating. However, the research about the application of flame retardant (FR) nanocomposites on RTS is still limited. As previously mentioned, RTS is also a special "cellulosic textile". Theoretically, the pyrolysis and combustion of RTS treated with FR nanocomposites should present lower burning temperature and tend to release less gaseous products.

In this work, FR nanocomposites including ST, DSP and HPDSP as "green" carbon source and APP as acid and gas source were added into tobacco concentrate to get modified-RTS by a paper-making process. Micro-scale combustion calorimetry (MCC), TG-FTIR and TG-MS have been used to study the influence of IFR on the thermal degradation, combustion behavior and the formation of evolved volatile products. In addition, the effect of IFR on temperature of burning cone has been investigated to evaluate the reduction of its flammability.

Experimental

Materials

Soluble ammonium polyphosphate ($n \leq 20$) was provided by Changsheng New Flame Retardant Co., Ltd (Shandong, China). Soluble starch was purchased from Sinopharm Group Chemical Reagent Co., Ltd (Shanghai, China). Distarch phosphate and hydroxypropyl distarch phosphate were purchased from Shuaishen Industrial Co., Ltd (Shanghai, China).

RTS and modified RTS were collected from China Tobacco Anhui Industrial Co. Ltd by a paper-making process.

Preparation of pure RTS and modified RTS

In the papermaking process, the raw materials of tobacco fines, dust, and stem were extracted with hot water followed by centrifugation, leaving behind a tobacco pulp and a tobacco extract. The tobacco extract was concentrated to adjust viscosity and volume. Meanwhile, the insoluble residue, mainly consisted of tobacco pulp and natural cellulose from wood, was mechanically smashed to reduce its fiber length. Then the tobacco based sheet was formed onto a web on the wire screen of a standard paper-making machine and dried by hot air and suction. Finally, the tobacco based sheet was immersed with the former concentrated tobacco extract and dried. For modified RTS, 1 kg APP and 1 kg ST were dissolved or dispersed into 40 L of concentrated tobacco extract to get the APP-ST-RTS sample (100 kg product). Similarly, APP-DSP-RTS and APP-HPDSP-RTS were made. As for control sample, only the former concentrated tobacco extract was added. The samples were conditioned at 22 °C and 60% relative humidity for at least 48 h. These RTS samples were handmade into cigarette samples with identical design features for cigarette burning cone analysis. The perimeter and length of cigarette samples were 24.5 mm and 84 mm, respectively. Prior to MCC, TG-FTIR and TG-MS analysis, the RTS samples were ground into powder to pass through an 80 mesh sieve for homogeneity.

SEM analysis

The morphology and element constituent of RTS and modified RTS were investigated using Schottky field-emission scanning electron microscopy (FE-SEM, Gemini 500, Zeiss, Germany).

Micro-scale combustion calorimetry

An "MCC-2" microscale combustion calorimeter (Govmark Organization Inc., Farmingdale, New York) was used to perform MCC tests. About 5 mg RTS sample was heated to a specified temperature (i.e. 650 °C) at a heating rate of 60 K min^{-1}, with a stream of nitrogen flow of 80 mL min^{-1}. The combustion

products were mixed with a flow of 20 mL min^{-1} O_2 before entering a combustion furnace set at 900 °C. Each sample was run in three replicates and the data presented here are the averages of the three measurements.

TG-FTIR analysis

TG-FTIR analysis was performed using TL-9000 thermogravimetric analyzer interfaced to the Nicolet 6700 FTIR spectrophotometer. About 10 mg of RTS sample powder was put in an alumina crucible and heated from 30 to 850 °C at a heating rate of 30 K min^{-1} under the flow of 20% oxygen in nitrogen. The pyrolysis products generated from the TGA furnace were introduced into the gas cell of the FTIR analyzer by nitrogen with a flow rate at 60 mL min^{-1}. The temperature of IR cell and transferred line from the TGA to the FTIR were maintained at 250 °C. The FTIR was operated with continuous scan mode covering 4000–500 cm^{-1} at a resolution of 4 cm^{-1}. All samples were run in duplicate and the average value was calculated. The temperature was reproducible to ± 1 K and the mass to ± 0.5%.

TG-MS analysis

TG-MS analysis was performed using TL-9000 thermogravimetric analyzer interfaced to the PerkinElmer Clarus 680/SQ8T GC–MS system. About 5 mg of RTS sample powder was put in an alumina crucible and heated from 30 to 850 °C at a heating rate of 30 K min^{-1} under the flow of Helium at 60 mL min^{-1}. The temperature of transfer line between TG-MS, chromatography column, ion source and eight port valve were all maintained at 250 °C. The MS was operated in the EI mode at 70 eV energy, performed by full scan mode covering 44–300 amu and selected ions of m/z = 17, 18, 28, 30, 44 and 58. All samples were run in duplicate and the average value was calculated. The temperature was reproducible to ± 1 K and the mass to ± 0.5%.

Analysis of cigarettes burning cone

A semi-automated thermocouple insertion system was used to measure the temperature distribution of cigarette during burning. In summary, 5–7 extremely fine thermocouples (0.254 mm diameter) were

inserted into the cigarette at different depths accurately (shown as in Fig. S1). The cigarette conditioned at 22 °C and 60% relative humidity for 48 h was held by an interface, connecting to the smoking machine. The smoking machine was operated under the ISO standard smoking mode (suction capacity 35 mL with interval 60 s and duration of 2 s) (ISO 4387 1991). The position of the thermocouples along the tobacco rod can be adjusted depending on research purpose. When puffs were in progress, the data were recorded according to certain frequency. Subsequently, the temperature contour map could be obtained through corresponding software treatment. Detailed information about device and process of treatment were described in previous article (Li et al. 2014).

Results and discussion

Morphology of RTS and coated RTS

The SEM images of RTS and modified nanocomposite RTS are presented in Fig. 1. It can be observed that tiny branched crystal and sphere exists on the surface of flaky structures, which are made of APP combined with starch or its derivatives. From the partial enlarged picture, it could be seen that the tiny crystal and sphere existing on the surface of modified RTSs was nanoparticle, whose size could be obtained from the scale of picture. When heated, these nanocomposite microparticles, acting as acid source, carbon source and gas source, react firstly on the surface of RTS fiber and form intumescent char to retard the further thermal degradation of RTS ingredients. However, it is hard to distinguish from one another of ST, DSP and HPDSP, since they have similar appearance after swelling.

Optimization of ratio of flame retardant

To optimize the proportion of starch-based nanocomposite coating, two factors need to be considered: the combustion behavior and taste of modified RTS. As high content of starch and its derivatives seriously affect the aroma quality of cigarette smoke and the viscosity of the composite tobacco extract solution, their content is always fixed at 1 wt% (Zhu et al. 2018). Additionally, the flame retardancy of IFR coating becomes poor when the content below 1 wt%. Therefore, the combustion behavior of modified-RTS

with APP from 0.5 to 2.0 wt% was studied (ST/DSP/HPDSP was 1 wt%). The heat release rate (HRR) and total heat release (THR) obtained from MCC analysis can reflect the flammability of samples, of which the peak value (PHRR) is often chosen to evaluate combustion behavior (Chen et al. 2014a). As shown in Fig. 2, there is a slight decrease of PHRR value at 1% APP addition. With further increase of APP proportion, there is an approximate platform of PHRR, demonstrating a very slight increase of flammability of modified RTS. In Fig. 2b, it can be clearly seen that there is no strong relation between THR value and the proportion of APP, especially with APP > 1.0%. In fact, the excessive APP covered on the surface of RTS would result in less compact coating and more harmful gas such as NH_3 in its combustion products (Zhou et al. 2013). Hence, the proportion of APP and starch and its derivatives in the coating were all set on 1 wt%.

The combustion behavior of RTS and modified RTS

To investigate the effect of different flame retardants on the combustion properties of RTS, the combustion behavior of RTS and three starch-based modified RTSs was studied. HRR curves of RTS and modified RTS are compared in Fig. 3. The corresponding parameters are listed in Table 1. As shown in Fig. 3, the heat release of pure RTS consists of three main stages. Firstly, small molecular main ingredients and volatile compounds start to degrade and produce fuel gases after 150 °C, resulting in the increase of HRR curve. Then the rapid rise is caused by the degradation of biopolymers such as cellulose, hemicellulose, lignin and pectin from RTS. Then, it reaches to the peak value (PHRR, 115.6 W/g) at 339.1 °C. Finally, the combustion of char release relative lower heat and curve ends at about 650 °C (Zhou et al.2013, 2017).

After incorporating starch-based flame retardant nanocomposite, the combustion behavior of modified RTS changes. Modified RTS release more heat below 200 °C, especially APP-ST-RTS and APP-HPDSP-RTS. This is caused by the catalysis of flame retardants. Above 200 °C, the HRR curves are almost parallel to that of pure RTS, reflecting the near overall suppression. The HRR value of modified RTS are all decreased as compared to pure RTS, demonstrating the restrained combustion behavior. Among them, PHRR of APP-DSP-RTS is decreased by 32.8%, much
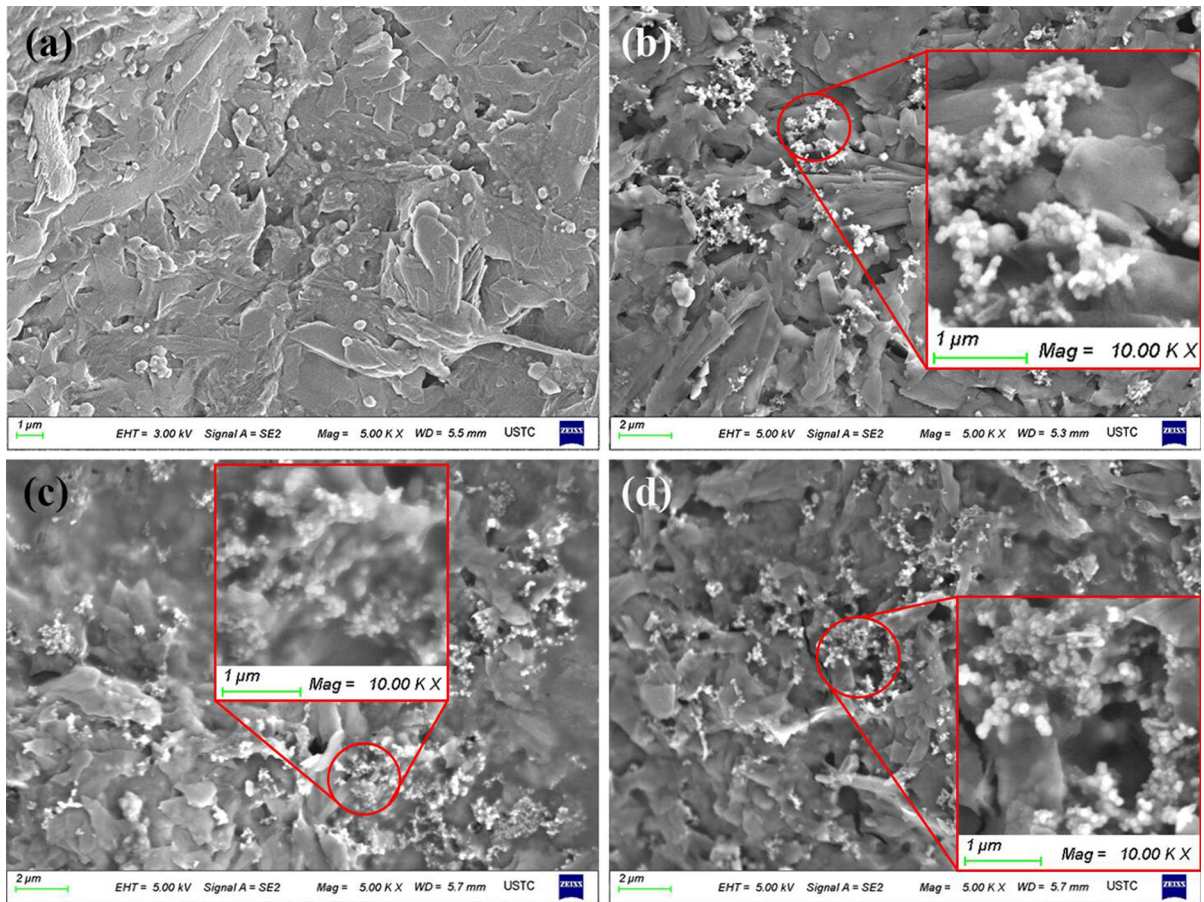
Fig. 1 SEM images of the surface of samples: **a** RTS, **b** APP-ST-RTS, **c** APP-DSP-RT and **d** APP-HPDSP-RTS
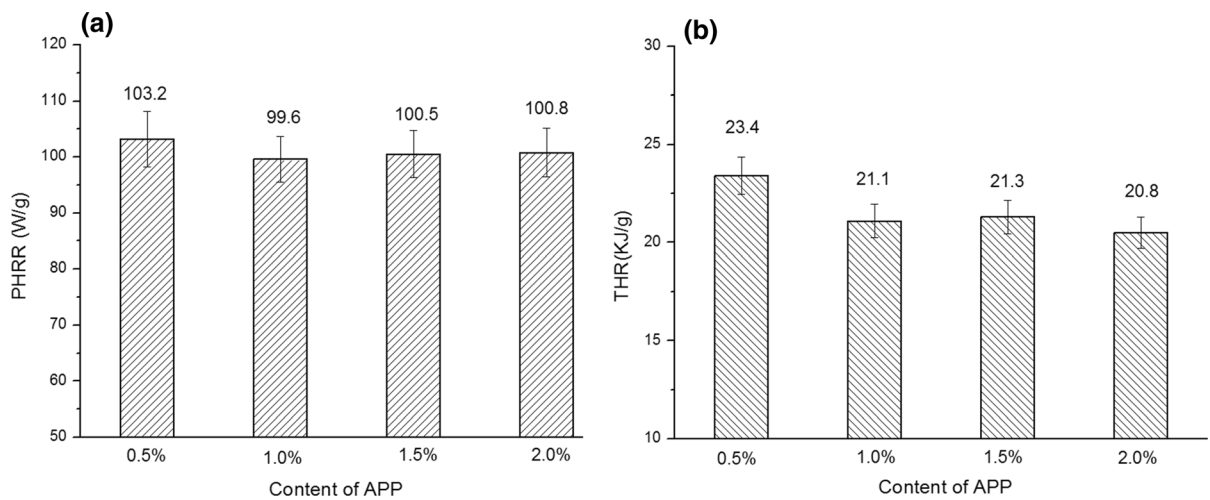

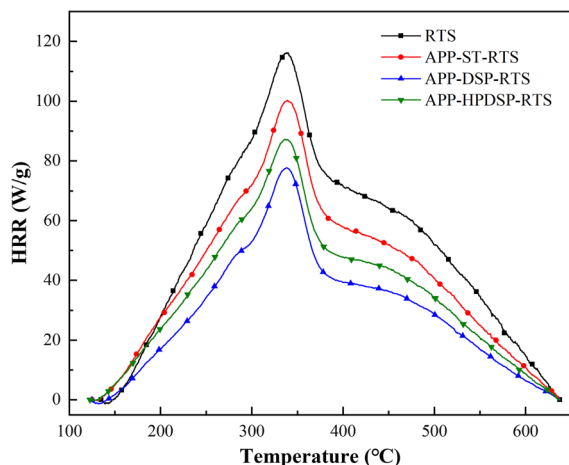**Fig. 2** The PHRR (**a**) and THR (**b**) of APP-ST-RTS coating with different contents of APP (ST: 1 wt%)

Fig. 3 HRR versus temperature curves of RTS and modified RTS

Table 1 MCC data of pure RTS and modified RTS

Sample	PHRR (W/g)	THR (kJ/g)	T_{PHRR} (°C)
RTS	115.6 ± 4.62	25.6 ± 0.17	339.1
APP-ST-RTS	99.6 ± 2.99	21.1 ± 0.15	337.8
APP-DSP-RTS	77.7 ± 2.33	15.1 ± 0.14	338.2
APP-HPDSP-RTS	87.2 ± 2.61	18.4 ± 0.14	336.9

greater than that of APP-ST-RTS (13.8%) and APP-HPDSP-RTS (24.6%). On the other hand, THR values show the similar trend, following the sequence of ST > HPDSP > DSP, which is identical to the trend

of R_2 (shown in Table 2). These results also prove the relative strength of flame retardancy for modified RTSs and indicate DSP present better inhibition on flame as a carbon source. Maybe DSP has more cross-linked phosphate ester groups interacted with APP and forms more stable char during combustion compared with HPDSP.

The thermal decomposition of RTS and modified RTS

To compare the effect of different carbon source on the thermal degradation of RTS and modified RTS, TG analysis was conducted. As shown in Fig. 4a and b, the thermal degradation of ST and its derivatives consists of three main stages. The minor mass loss below 160 °C is attributed to the evaporation of free water. Then, the glucose residues units of starch dehydrate to form an hydro-glucose and C–O, C–C bond, ring cleavage reactions bring about near 70% mass loss in 260–400 °C. Finally, the residual char formed earlier burns out at around 530 °C. Compared with ST, the R_1 and $T_{-50\%}$ values of DSP and HPDSP follow the order of ST > HPDSP > DSP, indicating the better thermal stability of modified starch. Moreover, the higher carbon content of ST brings higher M_f at 400 °C. In fact, there are two main zones in the "REAL" burning cigarette: the oxygen-enriched combustion zone located at the front and the oxygen-poor pyrolysis zone located at the back (Chen et al. 2014a). A series of complex chemical reactions, such as thermal decomposition, thermal synthesis and polymerization,
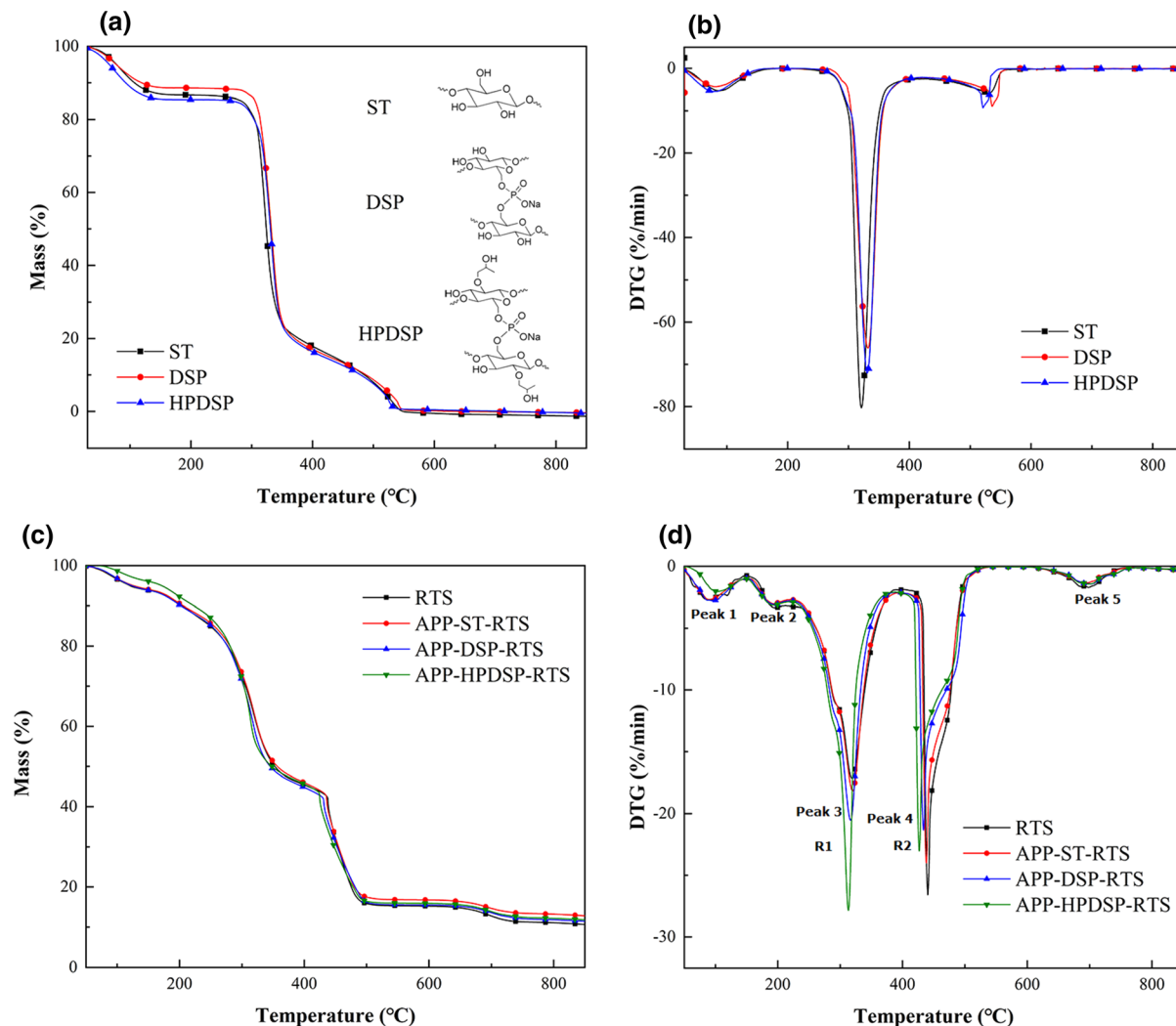
Table 2 Characteristic pyrolysis parameters of different carbon source and RTS samples

Sample	T_1^a (°C)	R_1^b (% min^{-1})	$T_{-50\%}^c$ (°C)	T_2^a (°C)	R_2^b (% min^{-1})	M_f^d (%)
ST	321.1	− 80.29	324.1	529.4	− 5.86	17.87
DSP	332.1	− 66.17	332.1	536.0	− 8.95	17.05
HPDSP	330.5	− 72.09	330.7	520.9	− 9.29	16.37
RTS	319.4	− 17.14	352.7	440.4	− 26.59	10.62
APP-ST-RTS	319.4	− 18.17	356.2	437.9	− 24.00	12.78
APP-DSP-RTS	316.7	− 20.54	345.3	434.0	− 21.35	11.42
APP-HPDSP-RTS	313.2	− 27.85	347.8	426.9	− 23.03	11.79

[a]The temperature according to Peak$_3$ (T_1) and Peak$_4$ (T_2)

[b]The maximum mass loss rate of Peak$_3$ (R_1) and Peak$_4$ (R_2)

[c]The temperature of 50% mass loss ($T_{-50\%}$)

[d]The mass of solid residue at 400 °C for carbon sources and 850 °C for RTS (M_f)

Fig. 4 TG and DTG curves of different carbon sources (**a**, **b**) and their modified RTSs (**c**, **d**)

occur in the pyrolysis distillation zone (oxygen-poor) of the organic compounds in tobacco, and are accompanied by the formation of products such as cigarette smoke and tar (Baker et al. 2004). Therefore, a constant air flow rate of 100 mL min^{-1} was chosen to imitate the real thermal degradation condition. The related parameters are listed in Table 2.

As for RTS, the decomposition of pure RTS consists of five stages. Firstly, the free water evaporates at 30–150 °C. Secondly, the volatile components such as small molecular carbonyl compounds escape at 150–220 °C. Thirdly, some main ingredients of RTS, such as cellulose, hemicellulose, lignin and pectin, decompose in 220–390 °C, accompanying the

formation of char. Then, the char burns at 390–520 °C rapidly. Finally, the inorganic salts, like $CaCO_3$ and $MgCO_3$, decompose at 620–760 °C, remaining 10.62% residue (Zhou et al. 2013; Ding et al. 2017).

When RTS is treated with APP-starch-based composite coating, the thermal degradation process has changed significantly. The main changes happen in the third and fourth stages. Firstly, at main ingredients decomposition stage, modified RTSs show more maximum mass lose rate and lower temperature range than pure RTS, indicating the decomposition is promoted. Among them, the T_1 value of modified RTSs follows the order of ST > DSP > HPDSP, and the R_1 follows the order of HPDSP > DSP > ST,

revealing that the contribution of flame retardants to char formation is consistent with HPDSP > DSP > ST. This is ascribed to cross-linked phosphate ester groups in the DSP and HPDSP. There are more phosphate ester groups decomposed in the lower temperature range, which accelerate the decomposition of cellulose and hemicellulose and char formation. It is notable that mass lose rate (R_1) of APP-HPDSP-RTS becomes much greater than APP-DSP-RTS, which may be related to the viscosity changes of tobacco concentrate. Additionally, the R_2 value follows the sequence of ST > HPDSP > DSP, which is as same as thermal stability of carbon sources. The slower char combustion process of modified RTS (R_2) shows the better thermal stability of char, indicating the effect of flame retardants. As for T_2, it keeps consistent with trend of T_1. Finally, the residual mass of APP-ST-RTS, APP-DSP-RTS and APP-HPDSP-RTS are 12.78%, 11.42% and 11.79%, which are all more than pure RTS. Among three starch-based IFR, both DSP and HPDSP have cross-linked phosphate ester group, which can produce more polyphosphoric acid in initial degradation stage and release more volatile gases at high temperature stages than that of APP-ST-RTS. Due to the relative more carbon forming agents, APP-ST-RTS leaves more residues.

According to above analysis, the starch-based FR nanocomposites have a significant effect on the thermal degradation of RTS. Because of promoting of the starch-based FR coating, there were more biopolymer complex chemical reactions occur in the pyrolysis to form more stable complex char layer. Obviously, the phosphate crosslinked starch-DSP and HPDSP, as carbon source, has better flame retardancy. Of three modified RTSs, APP-DSP flame retardant has the best performance, because of its lowest mass lose rate of char combustion.

FTIR analysis of evolved gases of RTS and modified RTS

TG is used to analyze the thermodynamic parameters of material decomposition under inert gases via mass change while FTIR and MS are often used to analyze the pyrolysis products via coupling with TG (Yang et al. 2019). To analyze the combustion products, the FTIR spectrum of RTS and modified RTS at T_2 (corresponding to Table 2) under air atmosphere is presented in Fig. 5. As for pure RTS, some
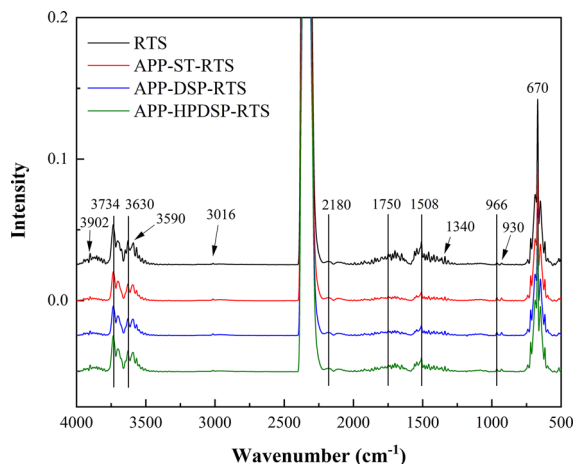

Fig. 5 FTIR spectrum of pyrolysis products of RTS and modified RTS at T_2 of the degradation

characteristic peaks belong to common gaseous products, such as water (3734 cm^{-1}), CO_2 (2358 and 670 cm^{-1}), CO (2180 and 2110 cm^{-1}), CH_4 (3016 cm^{-1}) and NH_3 (966 and 930 cm^{-1}) (Chen et al. 2015a). Besides, other absorption regions, like 1850–1630 cm^{-1} (carbonyl compounds) and 1600–1450 cm^{-1} (aromatic and alkene carbon) also reflect the generation of other compounds. The broad absorption band at 1450–1250 cm^{-1} can be ascribed to a series of C–O bond (Jin et al. 2016; Xu et al. 2019). After addition starch-based IFR nonocomposite, there is no obvious change about products species, while the relative intensity of some regions has decreased, such as 1850–1630 cm^{-1} and 1600–1250 cm^{-1}. This demonstrates the inhibition of IFR on the evolution of gaseous products.

Figure 6 displays the Gram–Schmidt (G–S) curves of total FTIR absorbance intensity and evolution curves of main volatiles, including H_2O (3734 cm^{-1}), CO (2180 cm^{-1}), CO_2 (2358 cm^{-1}), C=O (1750 cm^{-1}), NH_3 (966 cm^{-1}). Firstly, in the G–S curves, the thermal decomposition of cellulose, hemicellulose, lignin, pectin and combustion of char produce most of gases, while the contribution of water and volatile substances removal is very limited (Zhou et al. 2013). It is noteworthy the modified RTS produce less gases in 200–400 °C, but the mass lose rate are greater than pure RTS in TG curves. In this stage, faster degradation of modified RTSs forms more solid phase and less gas phase, which reveals the formation of intumescent char. Afterwards, the char
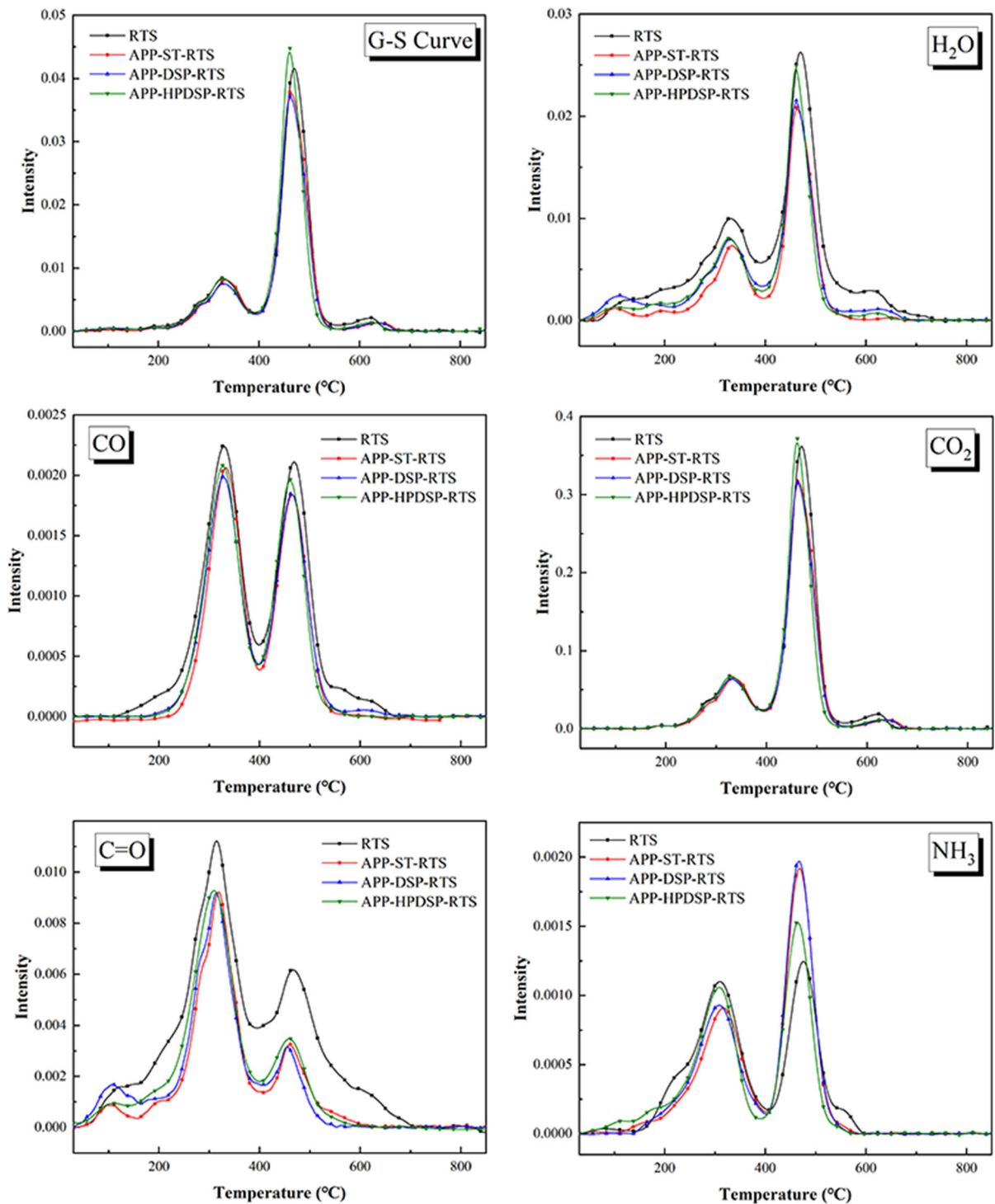
Fig. 6 The Gram-Schmidt curves of the total FTIR absorbance intensity of gaseous products and evolution of different gaseous production of RTS and modified RTS in TG-FTIR experiment

combustion generates plenty of gases, much more than inorganic salt decomposition stage. The formation of gaseous products is decreased by IFR in the whole temperature range, with the weakest intensity of APP-DSP-RTS.

As shown in Fig. 6, water, volatile carbonyl compounds and NH_3 are released out below 160 °C. With temperature increasing, main ingredients decompose and the various products generate rapidly and reach their peak value at the temperature of first maximum mass lose rate, especially CO and carbonyl compounds. Obviously, the intensity at peak temperature for modified RTS is weaker. When coming to char combustion, unlike H_2O, CO_2, CO, NH_3, the release of carbonyl compounds becomes relatively weaker as compared to former stage. Since the polysaccharides have been depolymerized, the reaction tends to full oxidation. Meanwhile, the release of CO is still a lot, which comes from the incomplete oxidation of char and reaction between char and huge amount of CO_2. The release of NH_3 primarily comes from the thermal decomposition of nitrogen-containing compounds in tobacco, such as protein, amino acid, amine salt, nicotine, nitrate and tobacco specific nitrosamines. The formation of NH_3 for modified RTS is much greater in char combustion stage, which reveals that these compounds are involved in char formation. Besides, the existence of APP can also release partial NH_3 in 400–600 °C. Therefore, as far as modified RTS is concerned, in addition to NH_3, the release of main products is promoted below 160 °C but inhibited during the char formation and combustion stages. The promotion at lower temperature reflects the catalytic effect of IFR. That may be attributed to that APP-starch-based nanocomposite coating decomposed earlier, producing polyphosphoric acid and releasing plenty of volatile gases at high temperature stages. The polyphosphoric acid promotes the dehydration of ST and its derivatives and formation of layer char on the surface of RTS, which separate the RTS materials from atmosphere and prevent the further decomposition. Among three starch-based IFR, in terms of harmful products like carbonyl compounds and CO, the DSP and HPDSP with cross-linked phosphate ester group present the relative better inhibition, which can produce more polyphosphoric acid in initial degradation stage.

TG-MS analysis of evolved gases of RTS and modified RTS

To elucidate the evolved products of degradation of RTS and modified RTS, further investigation was conducted using the coupling TG-MS. Figure 7 displays the total ion current curves and some single ion current curves of RTS and three starch-based modified RTSs, including m/z = 17, 18, 30, 44 and 58. It can be seen that the evolved gaseous products of RTS consists of three main stages in the TIC curves (Fig. 7a), which correspond to evaporation of small molecule (such as water, NH_3 and etc.), decomposition of biopolymer and char combustion. It is noteworthy there is a slow rise at 250–450 °C and then a rapid rise from 450 °C and reach their peaks about 520 °C in TIC curves which means RTS produce more gases in char combustion stage than decomposition of biopolymer stage. In decomposition of biopolymer stage, faster degradation of modified RTS forms more solid phase and less gas phase, which reveals the formation of intumescent char. In Fig. 7b and c, the peaks at m/z = 17, 18 which appear with strong intensity during three stages can be assigned to NH_3 and water, respectively. The mass per charge ratio, m/z = 28 corresponds mainly to CO, C_2H_4 and N_2. All the three can be expected from RTS sample (Ahamad and Alshehri 2012). In view of the low content of CO and interference of C_2H_4 and N_2, CO isn't displayed in picture. The release of CO_2 is confirmed by a fragment at m/z = 44 and it is also supported by FTIR data where carbon dioxide has been observed in second and third stages. The MS fragments for formaldehyde (m/z = 30), acetone (m/z = 58) and propionaldehyde (m/z = 58) show intensity at second and third stages during the degradation. These compounds all belong to the same groups of chemicals as carbonyl compounds which can cause cancer. In fact, acetaldehyde (m/z = 44) is also one of these carbonyl compounds but its ion current peak is masked by CO_2 whose content is much higher than its. In terms of harmful products like formaldehyde and acetone (Fig. 7d, f), the DSP and HPDSP with cross-linked phosphate ester group present the relative better inhibition, which can produce more polyphosphoric acid in initial degradation stage. This is in agreement with the TG-FTIR spectra. Moreover, as far as modified RTS is concerned, the release of main products is inhibited during whole thermal
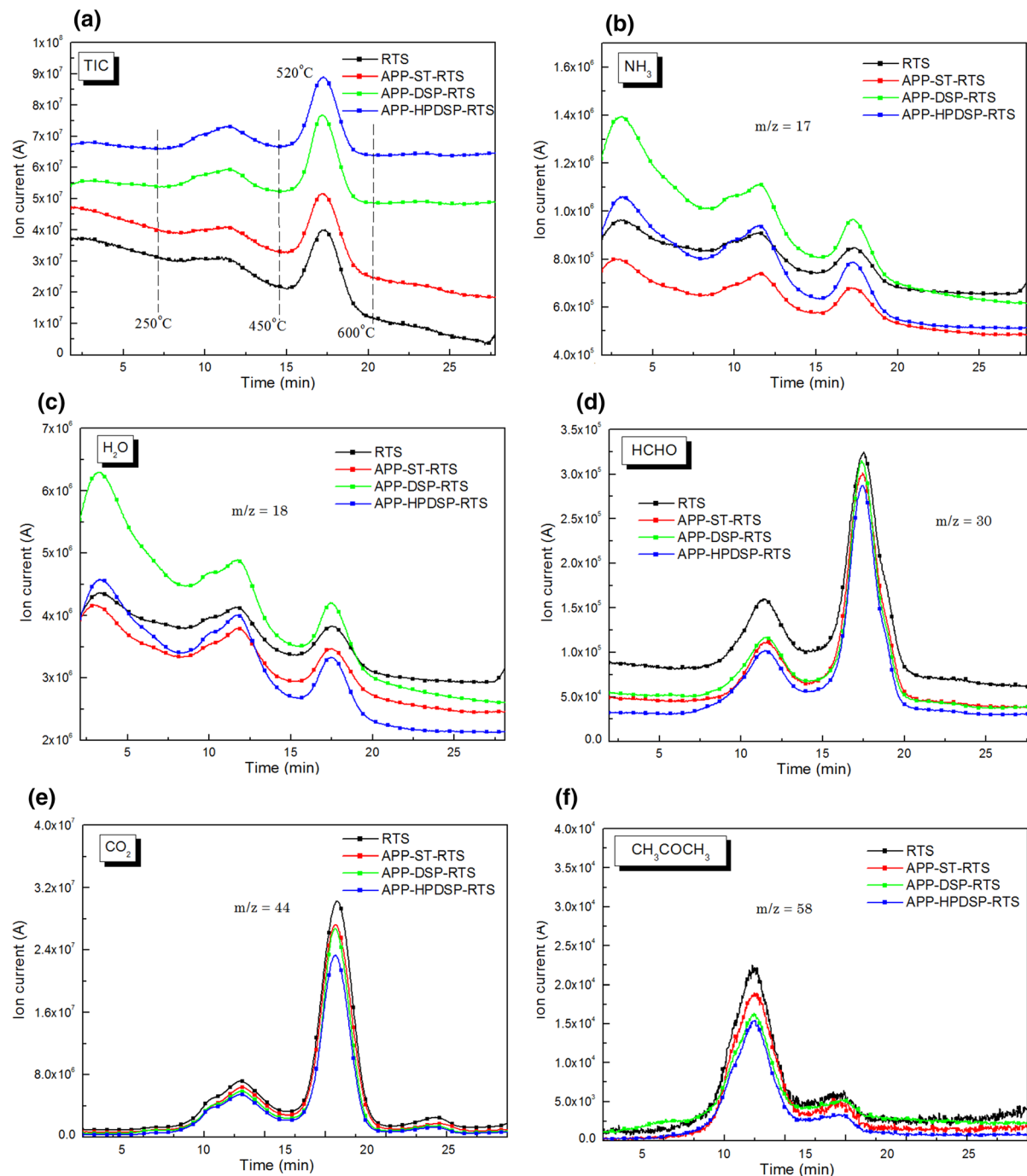
Fig. 7 Total ion current chromatogram and main single ion current chromatogram of pyrolysis products during thermal degradation of RTS and modified RTS

degradation stages, especially char combustion stage. That may be attributed to that APP-starch-based nanocomposite coating promotes the dehydration of ST and its derivatives and formation of char layer on the surface of RTS, which separate the RTS from atmosphere and prevent the further decomposition.
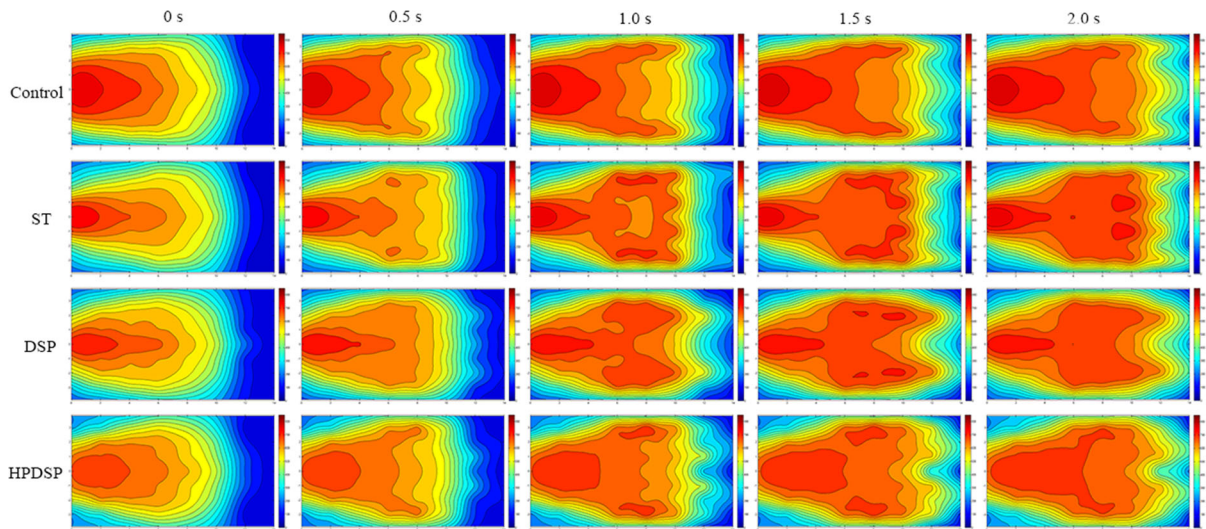
Fig. 8 The temperature contour map of cigarette burning cone for RTS and modified RTS

Burning cone characteristic analysis of cigarettes made from RTS and modified RTS

Figure 8 displays the temperature contour map of RTS cigarettes burning cone. The corresponding parameters, such as V_0, ABR, T_{max} and F, are listed in Table 3. It can be clearly seen that the burning cone shapes of modified RTS are slimmer than pure RTS at beginning and the average volume of APP-HPDSP-RTS (628.7 mm^3) is the smallest of four RTS samples. With start of the suction, a large amount of air enters the interior and reacts with RTS materials to accelerate combustion. The borderline of burning cone retreats quickly, while the center moves slowly. Meanwhile, burning cone volume and temperature increase rapidly and reach its maximum value at about 1.5 s. During static combustion and suction, the V_0, ABR, T_{max} all follow the sequence of RTS > ST > DSP > HPDSP, which also confirms the fire resistance of modified RTS. Actually, higher viscosity of HPDSP solution reduces density of APP-HPDSP-RTS, which can be concluded by the comparison of filling value (F) (Berski et al. 2011). For the same mass RTS in a cigarette, the interior of cigarette with bigger F value becomes more compact. Therefore, it is difficult for air to get into the cigarette interior, which caused the worst flammability of APP-HPDSP-RTS. Above analysis shows that IFR nanocomposite containing starch-based phosphate esters restrain combustion of RTS well, which is in good agreement with other results.

Table 3 Characteristic parameters of burning cone of cigarettes made from RTS and coated RTS

Sample	V_0^a (mm^3)	ABR^b (mm/s)	T_{max}^c (°C)	F^d (cm^3/g)
RTS	639.5 ± 1.7	0.1169 ± 0.035	796.0 ± 9.8	5.49 ± 0.25
APP-ST-RTS	637.0 ± 1.3	0.1083 ± 0.031	775.6 ± 10.1	5.66 ± 0.27
APP-DSP-RTS	632.9 ± 1.6	0.1048 ± 0.035	767.0 ± 7.6	5.61 ± 0.26
APP-HPDSP-RTS	628.7 ± 2.0	0.1018 ± 0.033	737.0 ± 8.4	5.71 ± 0.26

[a] The average volume of burning cone (V_0)

[b] The average burning rate (ABR)

[c] The maximum temperature of burning cone (T_{max})

[d] The filling value of RTS shreds (F), namely the volume of RTS shreds per gram

Conclusion

In this work, ST and its derivatives (DSP, HPDSP), as a series of most popular renewable and biodegradable polymers, were served as "green" carbon sources to prepare IFR nanocomposite materials applied on RTS. The thermal degradation and combustion behavior of modified RTS were studied in detail. Both MCC and TG analysis indicated that the cross-linked phosphate ester groups in carbon sources could improve the flame retardancy through promoting char formation and enhancing the dehydration ability. Therefore, APP-DSP-RTS (77.7 W/g), APP-HPDSP-RTS (87.2 W/g) and APP-ST-RTS (99.6 W/g) present lower PHRR values than that of pure RTS (115.6 W/g). Besides, FTIR and MS analysis of gaseous products shows that modified RTSs release relative less harmful compounds, such as CO and carbonyl compounds. Finally, the cigarette burning cone analysis demonstrated that modified RTSs had smaller burning cone volume, lower burning temperature and slower combustion rate than that of pure RTS, especially APP-HPDSP-RTS. Thus, the starch-based flame retardants nanocomposite is a feasible means to reduce the combustion temperature of cigarettes and health risks of smoking in tobacco industry. Our work provides a new insight into expending the application fields of starch and its derivatives.

Compliance with ethical standards

Conflict of interest The authors declare that they have no conflict of interest.

References

Ahamad T, Alshehri SM (2012) TG–FTIR–MS (evolved gas analysis) of bidi tobacco powder during combustion and pyrolysis. J Hazard Mater 199–200:200–208

Baker RR, Pereira da Silva JR, Smith G (2004) The effect of tobacco ingredients on smoke chemistry. Part I: flavourings and additives. Food Chem Toxicol 42:3–37

Berski W, Ptaszek A, Ptaszek P, Ziobro R, Kowalski G, Grzesik M, Achremowicz B (2011) Pasting and rheological properties of oat starch and its derivatives. Carbohyd Polym 83:665–671

Calabuig E, Juárez-Serrano N, Marcilla A (2019) TG-FTIR study of evolved gas in the decomposition of different types tobacco. Effect of the addition of SBA-15. Thermochim Acta 671:209–219

Chen M, Xu Z, Chen G, Ge S, Yin C, Zhou Z, Sun W, Li Y, Zhong F (2014a) The generation of carbon monoxide and carbonyl compounds in restituted tobacco sheet. J Therm Anal Calorim 115:961–970

Chen M, Xu Z, Chen G, Wang H, Yin C, Zhou Z, Sun W, Li Y, Zhong F (2014b) The influence of exogenous fiber on the generation of carbonyl compounds in reconstituted tobacco sheet. J Anal Appl Pyrol 105:227–233

Chen L, Wang X, Yang H, Lu Q, Li D, Yang Q, Chen H (2015a) Study on pyrolysis behaviors of non-woody lignins with TG-FTIR and Py-GC/MS. J Anal Appl Pyrol 113:499–507

Chen S, Li X, Li Y, Sun J (2015b) Intumescent flame retardant and self-healing superhydrophobic coatings on cotton fabric. ACS Nano 9:4070–4084

Chen J, Wang Y, Liu J, Xu X (2020) Preparation, characterization physicochemical property and potential application of porous starch: a review. Int J Biol Macromol 148:1169–1181

Deng S, Liao W, Yang J, Cao Z, Wang Y (2016) Flame-retardant and smoke-suppressed silicone foams with chitosan-based nanocoatings. Ind Eng Chem Res 55:7239–7248

Ding M, Wei B, Zhang Z, She S, Huang L, Ge S, Sheng L (2017) Effect of potassium organic and inorganic salts on thermal decomposition of reconstituted tobacco sheet. J Therm Anal Calorim 129:975–984

Gao W, Chen K, Yang R, Yang F (2015) Process for coating of reconstituted tobacco sheet with citrates. J Anal Appl Pyrol 114:138–142

Hamadache H, Djidjelli H, Boukerrou A, Kaci M, Antonio J, Martin-Martinez J (2019) Different compatibility approaches to improve the thermal and mechanical properties of EVA/starch composites. Polym Compos 40:3242–3253

ISO 4387 (1991) Cigarettes-determination of total and nicotine free dry particulate matter using a routine analytical smoking machine; Reference number ISO 4378:1991 (E). International organization for standardization, Geneva

Jin W, Shen D, Liu Q, Xiao R (2016) Evaluation of the co-pyrolysis of lignin with plastic polymers by TG-FTIR and Py-GC/MS. Polym Degrad Stab 133:65–74

Li B, Pang H, Zhao L, Wang B, Liu C, McAdam K, Luo D (2014) Quantifying gas-phase temperature inside a burning cigarette. Ind Eng Chem Res 53:7810–7820

Li X, Zhao Z, Wang H, Yan H, Zhang X, Xu B (2017) Highly efficient flame retardant, flexible, and strong adhesive intumescent coating on polypropylene using hyperbranched polyamide. Chem Eng J 324:237–250

Lin D, Zeng X, Li H, Lai X (2018) Facile fabrication of superhydrophobic and flame-retardant coatings on cotton fabrics via layer-by-layer assembly. Cellulose 25:3135–3149

Liu X, Zhang Q, Cheng B, Ren Y, Zhang Y, Ding C (2018) Durable flame retardant cellulosic fibers modified with novel, facile and efficient phytic acid-based finishing agent. Cellulose 25:799–811

Liu J, Dong C, Zhang Z, Kong D, Sun H, Lu Z (2020) Multifuction flame-retarded and hydrophobic cotton fabrics modfied with a cyclic phophorus/polysiloxane copolymer. Cellulose 27:3531–3549

Oltramari K, Madrona G, Neto A, Morais G, Baesso M, Bergamasco R, Moraes F (2017) Citrate esterified cassava starch: preparation, physicochemical characterisation. Starch/Stärke 69:1700044

Passauer L, Liebner F, Fischer K (2009) Starch phosphate hydrogels. PartI: synthesis by mono-phosphorylation and cross-linking of starch. Starch/Stärke 61:621–627

Safdari M, Amini E, Weise D, Fletcher T (2019) Heating rate and temperature effects on pyrolysis products from live wildland fuels. Fuel 242:295–304

Schirp A, Hellmann A (2019) Fire retardancy improvement of high-density polyethylene composites based on thermo-mechanical pulp treated with ammonium polyphosphate. Polym Compos 40:2410–2423

Shen J, Fatehi P, Ni Y (2014) Biopolymers for surface engineering of paper-based products. Cellulose 21:3145–3160

Shi Y, Wang G (2016) The novel epoxy/PEPA phosphate flame retardants: synthesis, characterization and application in transparent intumescent fire resistant coatings. Prog Org Coat 97:1–9

Takahashi Y, Kanemaru Y, Fukushima T, Eguchi K, Yoshida S, Miller-Holt J, Jonese I (2018) Chemical analysis and in vitro toxicological evaluation of aerosol from a novel tobacco vapor product: a comparison with cigarette smoke. Regul Toxicol Pharm 92:94–183

Talhout R, Schulz T, Florek E, Benthem J, Wester P, Opperhuizen A (2011) Hazardous compounds in tobacco smoke. Int J Environ Res Public Health 8:613–628

Wang Y, Chen K, Mo L, Li J, Xu J (2014) Optimization of coagulation-flocculation process for papermaking-reconstituted tobacco slice wastewater treatment using response surface methodology. J Ind Eng Chem 20:391–396

Wang X, Yuan Y, Yue T (2015) The application of starch-based ingredients in flavor encapsulation. Starch/Stärke 67:225–236

Wang W, Wen P, Zhan J, Hong N, Cai W, Gui Z, Hu Y (2017) Synthesis of a novel charring agent containing pentaerythritol and triazine structure and its intumescent flame retardant performance for polypropylene. Polym Degrad Stab 144:454–463

Wang D, Zhong L, Zhang C, Li S, Tian P, Zhang F, Zhang G (2019) Eco-friendly synthesis of a highly efficient phosphorus flame retardant based on xylitol and application on cotton fabric. Cellulose 26:2123–2138

Wang W, Guo J, Liu X, Li H, Sun J, Gu X, Wang J, Zhang S, Li W (2020) Constructiong eco-friendly flame retardant coating on cotton fabrics by layer-by-layer self-accembly. Cellulose 27:5377–5389

Xu F, Zhong L, Xu Y, Zhang C, Zhang F, Zhang G (2019) Highly efficient flame-retardant and soft cotton fabric prepared by a novel reactive flame retardant. Cellulose 26:4224–4240

Yan H, Li N, Cheng J, Song P, Fang Z, Wang H (2018) Fabrication of flame retardant benzoxazine semi biocomposites reinforced by ramie fabrics with bio-based flame retardant coating. Polym Compos 39(S1):E480–E488

Yang Z, Fu L, Fan F (2019) Thermal characteristics and kinetics of waste *Camellia oleifera* shells by TG-GC/MS. ACS Omega 4:10370–10375

Zeng F, Qin Z, Li T, Chen Y, Yang L (2020) Boosting phosphorus-nitrogen-silicon synergism through introducing graphene nanobrick wall structure for fabrication multifuctional cotton fabric by spray assisted layer-by-layer assembly. Cellulose 27:6691–6705

Zhang L, Xue W, Gu L (2020) Study on properties and application of pyrophosphate flame retardant microcapsules prepared from hemicellulose maleate. Cellulose 27:3931–3946

Zhao B, Kolibaba TJ, Lazar S, Grunlan JC (2020) Facile two-step phosphazine-based network coating for flame retardant cotton. Cellulose 27:4123–4132

Zhou S, Ning M, Xu Y, Hu Y, Shu J, Wang C, Ge S, Tian Z, She S, He Q (2013) Thermal degradation and combustion behavior of reconstituted tobacco sheet treated with ammonium polyphosphate. J Anal Appl Pyrol 100:223–229

Zhou S, He Q, Wang X, Ning M, Yang Y, Xu Y, Zhang Y, Zou P, Tian Z, Chen K, Wang H, She S (2017) An insight into the roles of exogenous potassium salts on the thermal degradation of flue-cured tobacco. J Anal Appl Pyrol 123:385–394

Zhu X, He Q, Hu Y, Huang R, Shao N, Gao Y (2018) A comparative study of structure, thermal degradation, and combustion behavior of starch from different plant sources. J Therm Anal Calorim 132:927–935